Reduction **Hot Paper**

Deutsche Ausgabe: DOI: 10.1002/ange.201603878
Internationale Ausgabe: DOI: 10.1002/anie.201603878

Hydrogenation of CO_2 to Formic Acid with a Highly Active Ruthenium Acriphos Complex in DMSO and DMSO/Water

*Kai Rohmann, Jens Kothe, Matthias W. Haenel, Ulli Englert, Markus Hölscher, and Walter Leitner**

Abstract: *The novel [Ru(Acriphos)(PPh_3)(Cl)($PhCO_2$)] [**1**; Acriphos = 4,5-bis(diphenylphosphino)acridine] is an excellent precatalyst for the hydrogenation of CO_2 to give formic acid in dimethyl sulfoxide (DMSO) and DMSO/H_2O without the need for amine bases as co-reagents. Turnover numbers (TONs) of up to 4200 and turnover frequencies (TOFs) of up to $260\,h^{-1}$ were achieved, thus rendering **1** one of the most active catalysts for CO_2 hydrogenations under additive-free conditions reported to date. The thermodynamic stabilization of the reaction product by the reaction medium, through hydrogen bonds between formic acid and clusters of solvent or water, were rationalized by DFT calculations. The relatively low final concentration of formic acid obtained experimentally under catalytic conditions ($0.33\,mol\,L^{-1}$) was shown to be limited by product-dependent catalyst inhibition rather than thermodynamic limits, and could be overcome by addition of small amounts of acetate buffer, thus leading to a maximum concentration of free formic acid of $1.27\,mol\,L^{-1}$, which corresponds to optimized values of $TON = 16\times10^3$ and $TOF_{avg} \approx 10^3\,h^{-1}$.*

The hydrogenation of carbon dioxide to formic acid has been intensively studied as an organometallic-catalyzed transformation of CO_2 for a long time.[1,2] The reaction has seen increasing interest recently because of the growing interest in the potential of CO_2 as either a raw material for chemical production or as an energy vector to store or harvest renewable energy via H_2.[3,4] The challenges to be met for these applications are related to the thermodynamic instability of formic acid relative to the gaseous starting materials and to the rate at which a given catalyst can shift the equilibrium to the desired direction [Scheme 1, Eq. (1)].[2a] While a variety of highly active molecular catalysts allowing turnover frequencies (TOFs) of several hundred thousand catalytic cycles per hour have been reported for the hydrogenation of CO_2 to formic acid, the reaction systems typically involve stoichiometric amounts of an amine or other strong bases as co-reagents.[3,5] Whereas the main role of the base can be associated with the enthalpic stabilization of the product by its conversion into formate salts or adducts [Scheme 1, Eq. (2)], there is also evidence that amine bases, in particular, can have a positive impact on the reaction rate. For example, they can be involved in the catalytic cycle by assisting the heterolytic hydrogen splitting for hydrogenolysis of the M−O bond in metal–formate intermediates.[6]

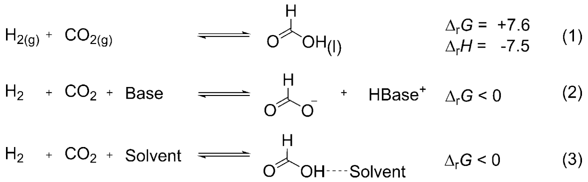

Scheme 1. Gibbs free energy (Δ_rG) and enthalpy (Δ_rH; all in kcal mol^{-1}) for the reaction of CO_2 and H_2 to formic acid [Eq. (1)]. The reaction is endergonic, however, the Gibbs free energy, Δ_rG, can be rendered exergonic by the addition of bases [Eq. (2)] or a stabilizing solvent [Eq. (3)].

In early studies, dimethylsulfoxide (DMSO) and water were identified as favorable solvents for CO_2 hydrogenation on the basis that hydrogen bonding would play an important role for the stabilization of formic acid [Scheme 1, Eq. (3)].[7] Although formation of free formic acid was observed in DMSO with the most active rhodium-phosphine catalysts at the time, concentrations remained low in contrast to the reaction conditions comprising additional amines. In 2014, Laurenczy et al. reported the first catalyst system allowing high concentrations of free formic acid in DMSO, in the absence of a base.[8] With the ruthenium complex [$Ru(Cl)_2(PTA)_4$] (PTA = 1,3,5-triaza-7-phosphaadamantane), turnover numbers (TONs) of up to 749 were achieved within 120 hours, thus resulting in a final HCOOH concentration of $1.9\,mol\,L^{-1}$ under optimized reaction conditions [$T = 60\,°C$ and $p°(H_2/CO_2, 1:1) = 100$ bar]. While this paper was under review, the group of Li reported an iridium complex which is capable of performing the base-free direct hydrogenation of CO_2 to form formic acid in water with a final concentration of $0.12\,mol\,L^{-1}$.[9] In the present contribution, we disclose a new

---

[*] M. Sc. K. Rohmann, M. Sc. J. Kothe, Dr. M. Hölscher, Prof. Dr. W. Leitner
Institut für Technische und Makromolekulare Chemie
Lehrstuhl für Technische Chemie und Petrolchemie
RWTH Aachen University
Worringerweg 2, 52074 Aachen (Germany)
E-mail: leitner@itmc.rwth-aachen.de

Prof. Dr. M. W. Haenel, Prof. Dr. W. Leitner
Max-Planck-Institut für Kohlenforschung
45470 Mülheim an der Ruhr (Germany)

Prof. Dr. U. Englert
Institut für Anorganische Chemie, RWTH Aachen University
Landoltweg 1, 52074 Aachen (Germany)

Supporting information and the ORCID identification number(s) for the author(s) of this article can be found under http://dx.doi.org/10.1002/anie.201603878.

base-free catalytic system which yields high concentrations of free formic acid with very high TOFs and TONs, thus providing additional insight into the interconnection of kinetic and thermodynamic control factors.

The precatalyst **1** was readily synthesized in 74% yield by stirring a toluene solution of $[Ru(PPh_3)_3(Cl)(PhCO_2)]$ (**2**)[10] and the Acriphos ligand[11] **3** for about 16 hours at 50 °C (Scheme 2). The rationale behind the design of **1** was to introduce the robust and very stable pincer-type coordination of **3**[12] into ruthenium-chloro-benzoate complexes, which were recently shown to provide efficient precursors for highly active hydrogenation catalysts.[13]

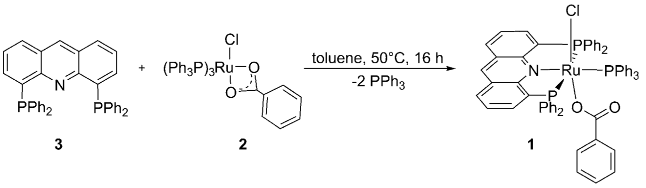

Scheme 2. Synthesis of **1** from **2** and **3**.

The molecular structure of **1** in the solid state was determined by single-crystal X-ray crystallography (Figure 1). The Acriphos ligand coordinates as expected, tridentate-meridionally with a P1-Ru-P2 angle of 160.5°. The benzoate ligand binds in a κ^1-mode, as one PPh_3 molecule of the starting complex completes the octahedral coordination geometry. The PPh_3 ligand is in a *trans* position to the N-donor in the Acriphos backbone. The $^{31}P\{^1H\}$ NMR spectrum of **1** shows a triplet at $\delta = 33.4$ and a doublet at $\delta = 39.7$ ppm with a coupling constant of 29.8 Hz, thus reflecting the trigonal planar arrangement of the three P-donor atoms. All analytical data (^1H, ^{13}C, and ^{31}P NMR spectroscopy, as well as mass spectrometry) are in accordance with the structure in the solid state and in solution (see the Supporting Information).

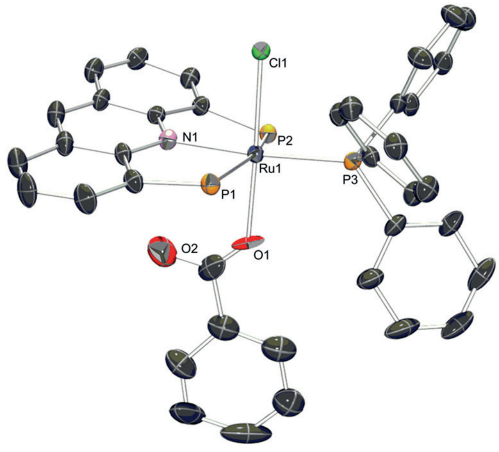

Figure 1. Structure of **1** in the crystal (thermal ellipsoids shown at 50% probability).[20] Hydrogen atoms as well as the phenyl rings of the Acriphos ligand were omitted for clarity. Selected atom distances [Å] and angles [°]: Ru1-P1 2.347, Ru1-P2 2.359, Ru1-P3 2.345, Ru1-O1 2.180, Ru1-N1 2.155, Ru-Cl1 2.441; P1-Ru-P2 160.54, O1-Ru1-P3 95.10.

The complex **1** was found to be active in the hydrogenation of CO_2 in DMSO, without any further additives, under mild standard reaction conditions (Table 1, entry 1). A formic acid concentration of 0.09 $mol\,L^{-1}$, corresponding to more than 10^3 catalytic turnovers, was determined by ^1H NMR spectroscopy in the reaction mixture after 16 hours. Thus an average TOF of 68 h^{-1} can be calculated as the lower limit for catalyst activity. Addition of small amounts of water of up to 5 vol% led to significantly higher end concentrations under otherwise identical reaction conditions, thus corresponding to a TON of 4×10^3 and average TOFs in the range of 250 h^{-1} (entries 2 and 3). Additional increase of the water content led to a decrease of productivity (entry 4), and finally to almost negligible formation in aqueous solution with small amounts of DMSO to solubilize the catalyst (entry 5).

Table 1: Hydrogenation of CO_2 to formic acid in DMSO/H_2O mixtures using **1** as a catalyst.

Entry[a]	Solvent	c (HCOOH) [mol L^{-1}]	TON	TOF_{av} [h^{-1}]
1	DMSO (5 ppm H_2O)	0.09	1094	68
2	97.5% DMSO 2.5% Water	0.31	4020	250
3	95% DMSO 5% Water	0.33	4200	260
4	90% DMSO 10% Water	0.14	1750	110
5	15% DMSO 85% Water	0.007	85	5

[a] Reaction conditions: 0.23 μmol [Ru], 80 bar H_2, 40 bar CO_2 (pressure at room temperature), 60 °C, 16 h, 3.0 mL total solvent volume. TONs and TOFs are mean values from at least two independent experiments with a mean deviation of ± (5–10) %. TOF_{av} is the average TOF over the full reaction time, thus defining a lower limit for the maximum activity of the catalyst.

The TONs and $TOFs_{av}$ observed with **1** in DMSO/H_2O (95:5 v/v; Table 1, entry 3) define the highest productivities and catalytic activities for amine-free hydrogenation of CO_2 to date. However, the observed concentration of free formic acid of 0.33 $mol\,L^{-1}$ is significantly lower than in the experiments of Dyson and Laurenczy,[8] who reported up to six-times higher concentrations under very similar reaction conditions. If reactions were carried out in the present system under addition of 0.16 $mol\,L^{-1}$ HCOOH at the beginning of the reaction, the final concentration was still 0.33 $mol\,L^{-1}$ after 16 hours. Even more significantly, no further increase of the formic acid concentration was detected within experimental error when 0.33 $mol\,L^{-1}$ HCOOH were added to the reaction mixture. This result clearly indicates that the maximum productivity that can be achieved with the catalyst system is limited by the final formic acid concentration, which does, however, not seem to reach the optimum concentration determined by thermodynamics in the reaction medium.

To get a more detailed understanding of the thermodynamic driving force for the stabilization of the product, DFT calculations were carried out to elucidate the interactions with DMSO and DMSO/water media. Detailed experimental studies have revealed the structure of the hydrogen-bonded adducts of formic acid with moderately to weakly basic tertiary amines,[14] which are the standard stabilizers used so far. Given the well-established role of DMSO as a hydrogen-bond acceptor, it is plausible to assume that similar adducts are formed with the solvent molecules in the absence of a base. Indeed, a stable 1:1 adduct of HCOOH and DMSO could be identified and structurally optimized, using the density functional MN12-L[15] developed by the group of Truhlar, with a basis set typically used for quantitative conclusions (def2-TZVP[16]). However, the enthalpic contribution of the hydrogen bond in the adduct was found to be too small to compensate for the unfavorable entropic contribution when using an implicit solvent model (see the Supporting Information). To model the solution-phase process more realistically, the adduct, as well as the reactants, were embedded in an explicit solvent cloud of 10 DMSO molecules and optimized using an implicit solvent model (IEF-PCM;[17] SMD,[18] see the Supporting Information for details).

The optimized structure of the hydrogen-bonded adduct in the solvent cloud is shown on the left-hand side of Figure 2.

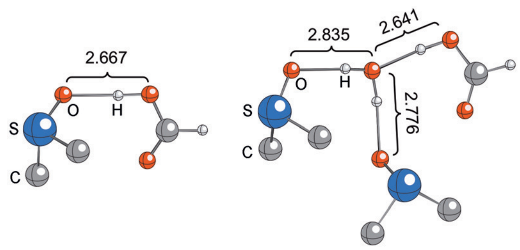

Figure 2. Core structures of the hydrogen-bonded adducts in the calculated clusters of formic acid in DMSO-based media as shown in Equations (4) [left] and (5) [right] (MN12-L/def2-TZVP(IEF-PCM, SMD)) with selected O–O distances [Å] highlighting the hydrogen bridges. The hydrogen atoms of the DMSO molecules were omitted for clarity as well as the other DMSO molecules of the solvent cloud. S, C, O, and H atoms are shown in decreasing size.

The hydrogen bridge between the proton of the carboxylate group of formic acid and the oxygen atom of the solvent molecule is clearly evidenced by the O–O distance of 2.67 Å, which is significantly shorter than the sum of the van der Waals radii of two oxygen atoms (3.1 Å). The formation of this adduct is weakly exergonic relative to the solvated starting materials when a solvent cluster of 10 DMSO molecules is considered [$\Delta_rG = -0.3$ kcal mol^{-1}; Scheme 3, Eq. (4)]. The computed Gibbs free energy of the reaction is even slightly more negative ($\Delta_rG = -0.6$ kcal mol^{-1}) when larger clusters of 20 DMSO molecules are considered.

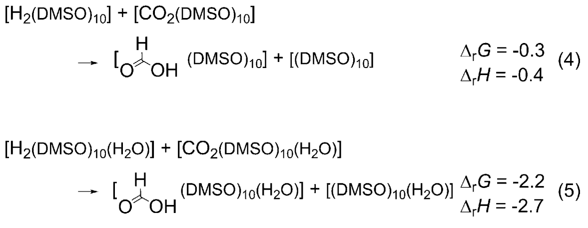

$$[H_2(DMSO)_{10}] + [CO_2(DMSO)_{10}] \rightarrow [HCOOH(DMSO)_{10}] + [(DMSO)_{10}] \quad \Delta_rG = -0.3 \quad \Delta_rH = -0.4 \quad (4)$$

$$[H_2(DMSO)_{10}(H_2O)] + [CO_2(DMSO)_{10}(H_2O)] \rightarrow [HCOOH(DMSO)_{10}(H_2O)] + [(DMSO)_{10}(H_2O)] \quad \Delta_rG = -2.2 \quad \Delta_rH = -2.7 \quad (5)$$

Scheme 3. Computed (MN12-L/def2-TZVP, IEF-PCM, SMD) Gibbs free energies (Δ_rG) and enthalpies (Δ_rH; all in kcal mol^{-1}) for the hydrogenation of CO_2 in DMSO and DMSO/H_2O solvent clouds.

Changing the solvent cloud to DMSO/H_2O in a ratio 10:1 resulted in an even larger driving force with a Gibbs free energy of reaction, Δ_rG, of -2.2 kcal mol^{-1} [Scheme 3, Eq. (5)]. This value can be associated with an increased stabilization resulting from the formation of three hydrogen bridges between DMSO, water, and formic acid (Figure 2, right). These computational results provide an analytical rationale for the thermodynamic stabilization of HCOOH in these media. They are also in agreement with the experimental results shown in entries 1–5 of Table 1, where the presence of small amounts of water led to a significant increase of the concentration of formic acid in the reaction mixture as compared to pure DMSO.

The significant Gibbs free energies of reaction calculated for the realistic solvent models furthermore substantiate the experimental evidence that the maximum amount of formic acid of 0.33 mol L^{-1} obtained in the DMSO/H_2O system is not limited by the thermodynamic equilibrium, but rather by the kinetic inhibition of **1** at this product concentration. An obvious parameter which might explain the product inhibition is the increasing proton concentration in solution resulting from the formation of HCOOH ($pK_a = 3.77$). Ruthenium hydride complexes, plausibly inferred as catalytic active species in CO_2 hydrogenation, are well known to be readily protonated, thus resulting in equilibria between neutral and cationic complexes.[19] To probe this hypothesis, reactions were carried out under standard reaction conditions, but in the presence of acetate buffer (CH_3COOH/CH_3COONa 1:1, pH 4.75).

Table 2: Hydrogenation of CO_2 to formic acid in buffered DMSO/H_2O mixtures using **1** as the precatalyst.

Entry[a]	Additive (mol L^{-1})	c (HCOOH) [mol L^{-1}]	TON	TOF$_{av}$ [h^{-1}]
1[b]	Acetate buffer (0.2)	1.03	13240	827
2[b]	Acetate buffer (0.4)	1.27	16310	1019
3	Acetic acid (0.16)	0.55	7040	423
4	Acetic acid (0.33)	0.61	8090	505
5	Acetic acid (0.66)	0.83	10680	670
6	Acetic acid (1.33)	0.79	10190	640

[a] Reaction conditions: 0.23 μmol [Ru], 80 bar H_2, 40 bar CO_2 (pressure at room temperature), 60 °C, 16 h, 3.0 mL total volume (5% H_2O), mean TONs and TOFs from at least two experiments with a deviation of ±(5–10)%. [b] 0.3 mL aqueous acetate buffer of 2.0 mol L^{-1} (entry 1) and 4.0 mol L^{-1} (entry 2) concentration, 3.0 mL total volume (10% H_2O).

As shown in Table 2, the catalytic hydrogenation in the buffered solution led indeed to a nearly fourfold increase in the final formic acid concentration, thus reaching up to 1.3 mol L^{-1} (entries 1 and 2), which is roughly six-times higher than the buffer concentration. The productivity of this system amounts to a TON of 16 310 and the observed TOF$_{av}$ indicates maximum turnover rates well above 1 000 h^{-1}. This performance is now approaching that of amine-based systems. As the molar ratio of HCOOH to sodium acetate is greater than 6:1, it can be ruled out that the buffer is acting merely as base to shift the thermodynamic equilibrium. This was further substantiated by using acetic acid alone as weak acid ($pK_a = 4.75$) to act as proton buffer. Although it was less effective than in combination with sodium acetate, it still resulted in a more than a twofold increase of the TONs and $TOFs_{av}$ of the catalytic system as compared to pure DMSO (entries 3–6).

In summary the complex **1** was shown to be a highly active precatalyst for the hydrogenation of CO_2 to give formic acid in the absence of amine bases. The productivity of the transformation is critically determined by a combination of thermodynamic and kinetic boundaries. Hydrogen bonding between HCOOH and the Lewis-basic solvent molecules, and the role of solvent clusters were determined as crucial factors in providing the necessary thermodynamic driving force for high equilibrium concentration of formic acid. These high concentrations can be achieved, however, only if the catalyst remains active over a wide range of proton concentrations. Considering the molecular active species and the reaction medium as an integrated catalytic system is therefore essential in the rational optimization of the process. Thus, catalytic turnovers as high as 4200 with average TOFs of $260\,h^{-1}$ could be achieved in DMSO/H_2O (95:5 v/v), and improved in buffered solutions to TONs of 16×10^3 and TOFs of $10^3\,h^{-1}$ at final formic acid concentrations of $1.3\,mol\,L^{-1}$. These data define one of the currently most productive and active catalytic systems for the hydrogenation of CO_2 to formic acid in the absence of bases as co-reagents.

Acknowledgments

This work was carried out within the framework of the International Research Training Group IRTG-1628 "Selectivity in Chemo and Biocatalysis (SeLeCa)", which is funded by the German Research Foundation.

Keywords: carbon dioxide · density functional calculations · hydrogenation · P ligands · ruthenium

How to cite: *Angew. Chem. Int. Ed.* **2016**, *55*, 8966–8969
Angew. Chem. **2016**, *128*, 9112–9115

---

[1] Y. Inoue, H. Izumida, Y. Sasaki, H. Hashimoto, *Chem. Lett.* **1976**, *5*, 863–864.
[2] a) W. Leitner, *Angew. Chem. Int. Ed. Engl.* **1995**, *34*, 2207–2221; *Angew. Chem.* **1995**, *107*, 2391–2405; b) P. G. Jessop, T. Ikariya, R. Noyori, *Chem. Rev.* **1995**, *95*, 259–272.
[3] a) P. G. Jessop, F. Joó, C.-C. Tai, *Coord. Chem. Rev.* **2004**, *248*, 2425–2442; b) C. Federsel, R. Jackstell, M. Beller, *Angew. Chem. Int. Ed.* **2010**, *49*, 6254–6257; *Angew. Chem.* **2010**, *122*, 6392–6395; c) M. Grasemann, G. Laurenczy, *Energy Environ. Sci.* **2012**, *5*, 8171–8181; d) W.-H. Wang, Y. Himeda, J. T. Muckerman, G. F. Manbeck, E. Fujita, *Chem. Rev.* **2015**, *115*, 12936–12973; e) J. Klankermayer, S. Wesselbaum, K. Beydoun, W. Leitner, *Angew. Chem. Int. Ed.* **2016**, *55*, 7296–7343; *Angew. Chem.* **2016**, *128*, 7416–7467.
[4] a) G. Centi, E. A. Quadrelli, S. Perathoner, *Energy Environ. Sci.* **2013**, *6*, 1711–1731; b) M. Aresta, A. Dibenedetto, A. Angelini, *Chem. Rev.* **2014**, *114*, 1709–1742; c) J. Klankermayer, W. Leitner, *Philos. Trans. R. Soc. London Ser. A* **2016**, *374*, DOI: 10.1098/rsta.2015.0315.
[5] a) R. Tanaka, M. Yamashita, K. Nozaki, *J. Am. Chem. Soc.* **2009**, *131*, 14168–14169; b) R. Tanaka, M. Yamashita, L. W. Chung, K. Morokuma, K. Nozaki, *Organometallics* **2011**, *30*, 6742–6750; c) C. A. Huff, M. S. Sanford, *ACS Catal.* **2013**, *3*, 2412–2416; d) G. A. Filonenko, R. van Putten, E. N. Schulpen, E. J. Hensen, E. A. Pidko, *ChemCatChem* **2014**, *6*, 1526–1530.
[6] a) F. Hutschka, A. Dedieu, M. Eichberger, R. Fornika, W. Leitner, *J. Am. Chem. Soc.* **1997**, *119*, 4432–4443; b) Y. Musashi, S. Sakaki, *J. Am. Chem. Soc.* **2000**, *122*, 3867–3877.
[7] a) E. Graf, W. Leitner, *J. Chem. Soc. Chem. Commun.* **1992**, 623–624; b) W. Leitner, E. Dinjus, F. Gaßner, *J. Organomet. Chem.* **1994**, *475*, 257–266.
[8] S. Moret, P. J. Dyson, G. Laurenczy, *Nat. Commun.* **2014**, *5*, 4017.
[9] S.-M. Lu, Z. Wang, J. Li, J. Xiao, C. Li, *Green Chem.* **2016**, DOI: 10.1039/c1036gc00856a.
[10] M. Hirano, R. Fujimoto, K. Hatagami, N. Komine, S. Komiya, *ChemCatChem* **2013**, *5*, 1101–1115.
[11] a) S. Hillebrand, Ph.D. thesis, Heinrich Heine University, Düsseldorf, **1996**; b) S. Hillebrand, B. Bartkowska, J. Bruckmann, C. Krüger, M. W. Haenel, *Tetrahedron Lett.* **1998**, *39*, 813–816.
[12] M. W. Haenel, S. Oevers, K. Angermund, W. C. Kaska, H. J. Fan, M. B. Hall, *Angew. Chem. Int. Ed.* **2001**, *40*, 3596–3600; *Angew. Chem.* **2001**, *113*, 3708–3712.
[13] a) A. B. Chaplin, P. J. Dyson, *Inorg. Chem.* **2008**, *47*, 381–390; b) K. Rohmann, M. Hölscher, W. Leitner, *J. Am. Chem. Soc.* **2016**, *138*, 433–443.
[14] K. Wagner, *Angew. Chem. Int. Ed. Engl.* **1970**, *9*, 50–54; *Angew. Chem.* **1970**, *82*, 73–77.
[15] R. Peverati, D. G. Truhlar, *Phys. Chem. Chem. Phys.* **2012**, *14*, 13171–13174.
[16] a) A. Schäfer, C. Huber, R. Ahlrichs, *J. Chem. Phys.* **1994**, *100*, 5829–5835; b) F. Weigend, R. Ahlrichs, *Phys. Chem. Chem. Phys.* **2005**, *7*, 3297–3305.
[17] a) E. Cancès, B. Mennucci, J. Tomasi, *J. Chem. Phys.* **1997**, *107*, 3032–3041; b) J. Tomasi, B. Mennucci, R. Cammi, *Chem. Rev.* **2005**, *105*, 2999–3094.
[18] A. V. Marenich, C. J. Cramer, D. G. Truhlar, *J. Phys. Chem. B* **2009**, *113*, 6378–6396.
[19] See for example: T. vom Stein, M. Meuresch, D. Limper, M. Schmitz, M. Hölscher, J. Coetzee, D. J. Cole-Hamilton, J. Klankermayer, W. Leitner, *J. Am. Chem. Soc.* **2014**, *136*, 13217–13225, and references therein.
[20] CCDC 1484129 (**1**) contain the supplementary crystallographic data for this paper. These data can be obtained free of charge from The Cambridge Crystallographic Data Centre.

Received: April 21, 2016